

LOW TEMPERATURE DOPING OF NIOBIUM CAVITIES: WHAT IS REALLY GOING ON?*

P. N. Koufalís[†], J. T. Maniscalco, M. Liepe, Cornell University, Ithaca, NY, USA

Abstract

It was first discovered at Fermilab, and subsequently replicated at Cornell, that low temperature heat treatments (120 – 160 °C) of niobium cavities in a low pressure atmosphere (20 – 60 mTorr) of nitrogen can lead to the so-called ‘ Q -rise’ and high Q_0 similar to that of cavities nitrogen-doped at high temperatures (~800 °C). It was suggested by Fermilab that the low temperature baking effect observed (i.e. Q -rise and high Q_0) was a result of nitrogen ‘infusion’ in the first ~5 nm of the niobium surface. We conducted a systematic study of the low temperature baking effect using RF measurements of a cavity prepared with a low temperature treatment as well as detailed secondary ion mass spectroscopy measurements of single-crystal niobium samples treated with various temperatures, durations, and gas mixtures. We demonstrate that the low-temperature baking is, in fact, drastically lowering the electron mean free path in the RF penetration layer, and that this is not primarily due to nitrogen ‘infusion’. Instead, it is shown that the diffusion and presence of other interstitial impurities (specifically carbon and oxygen) at high concentrations are the cause of the reduction in mean free path and, therefore, of the observed Q -rise and high Q_0 values.

INTRODUCTION

Many previous experiments have shown that niobium cavities doped with nitrogen at high temperature (~800 °C) leads to higher quality factors, Q_0 , and an increase of Q_0 with increasing gradients, E_{acc} [1, 2]. This effect is often to referred to as ‘anti- Q -slope’ or ‘ Q -rise’ [1]. Both effects result in lower cryogenic power loads reducing operating costs.

More recently it was discovered that cavities treated in a low temperature (~160 °C), low pressure (~40 mTorr) nitrogen atmosphere exhibited the same effects as cavities doped at high temperatures [3]. In this temperature regime, nitrogen only diffuses a few nm into the niobium surface over the course of a day whereas at higher temperatures (~800 °C) nitrogen is able to diffuse several μm into the surface within minutes. The observed effects in low temperature doped cavities were attributed to the presence of nitrogen in the first ~2 nm [4] and came to be called nitrogen ‘infusion’ [5]. However, it has been shown that nitrogen is not present in sufficient quantities to account for the observed Q -rise [6]. We demonstrate that it is other interstitial impurities (i.e. carbon and oxygen) that is responsible for the reduction of the mean free path and, therefore, of the observed effects.

Four TESLA-shaped [7] 1.3 GHz cavities received surface treatments summarized in Table 1 with Q_0 vs. E_{acc}

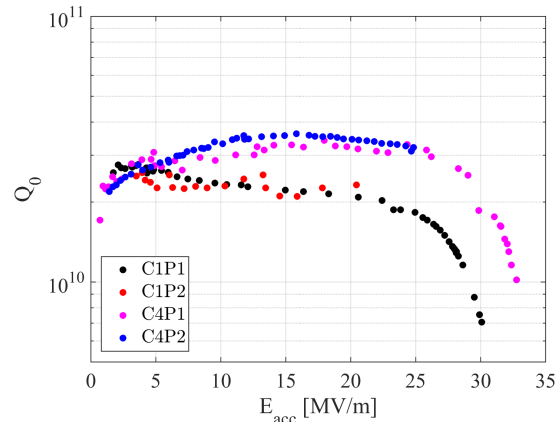


Figure 1: RF cavity performance for TESLA-shaped 1.3 GHz cavities at $T = 2.0$ K for a high temperature nitrogen doped cavity, a low temperature doped cavity, and two standard-treatment bulk-niobium cavities. Q -rise is observed for both the low temperature and high temperature doped cavities.

measurements shown in Fig. 1. Each cavity received electropolishing (EP) and high pressure rinsing (HPR) with de-ionized water before heat treatment.

HIGH TEMPERATURE NITROGEN DOPING

By introducing interstitial nitrogen to the niobium lattice the density of potential scattering sites increases and consequently the electron mean free path, ℓ , is reduced [2]. It has been experimentally observed that higher concentrations of nitrogen correspond to shorter mean free paths. The ‘strength’ of the Q -rise correlates strongly with the decrease in mean free path thus making ℓ a useful material parameter for quantifying the doping level [2]. Recent theoretical work by Gurevich [8] and experimental work by Maniscalco [9] provide a promising insight into the physical mechanism that leads to the observed effects in doped cavities.

In the high-temperature nitrogen-doping process the niobium cavity is heated treated in a low-pressure (~40 mTorr) nitrogen atmosphere at temperatures from 600-1000 °C. Niobium nitrides form on the surface of the cavity at these temperatures, allowing nitrogen to diffuse from the nitride into the bulk preferentially occupying octahedral interstitial sites [1, 2, 10]. Treatments may or may not include an annealing step in ultra-high vacuum after doping. Following heat treatment, the cavity receives an EP to remove the lossy nitride layer. We will see that low temperature doped cavities do not require post-doping EP.

* Work supported by NSF Award PHYS-1416318.

[†] pnk9@cornell.edu

Table 1: Cavity Surface Treatments

| Cavity | De-gas | Dope | Anneal |
|--------|---------------------|----------------------------------|----------------------|
| C1P1 | 900 °C (3 hr; UHV) | — | — |
| C1P2 | 800 °C (5 hr; UHV) | — | — |
| C4P1 | 800 °C (3 hr; UHV) | 800 °C (20 min; N ₂) | 800 °C (30 min; UHV) |
| C4P2 | 800 °C (10 hr; UHV) | 160 °C (48 hr; N ₂) | 160 °C (168 hr; UHV) |

In Fig. 1, the Q_0 as a function of E_{acc} for cavity C4P1 can be seen. This cavity was treated at 800 °C for 20 min in high purity nitrogen followed by a 30 min anneal in ultra-high vacuum. Following the doping procedure, the cavity received a 24 μm EP. The Q -rise and high Q_0 are quite typical of high temperature nitrogen doped cavities. The maximum field reached ~ 33 MV/m and was limited by the available input RF power rather than by thermal quench, field emission, or multipacting. It is typical for heavily nitrogen doped cavities to have stronger Q -rise and smaller quench fields, on average, and quench limitations can vary from a few up to 45 MV/m depending on the particular surface treatment [2].

LOW TEMPERATURE DOPING

During the low temperature doping process, the cavity first undergoes a degas at 800 °C for several hours (~ 3 –12 hr) and is then immediately cooled to low temperatures (100 – 200 °C). When it cools to the desired temperature, the cavity is exposed to a low pressure atmosphere (~ 40 mTorr) of continuously flowing high purity nitrogen for 24 to 96 hr. An additional annealing step in ultra-high vacuum may or may not be included. Other gas mixtures can be used, such as argon gas mixed with carbon dioxide. It is important that the atmosphere be continuously flowing so that trace impurities are constantly being replenished.

The performance of C4P2 is shown in Fig. 1. Initially, the cavity received a heavy 150 μm EP to smooth the surface and to remove any defects or impurities from previous treatments. It then received a heat treatment consisting of a degas at 800 °C for 10 hr followed immediately by a 160 °C bake in nitrogen for 48 hr. An anneal in ultra-high vacuum for 168 hr concluded the bake. No post-treatment EP was done. The temperature and pressure profiles during the bake are shown in Fig. 2.

RF MEASUREMENTS

The performance of C4P2 was very similar to that of the high temperature nitrogen doped cavity, C4P1. It possessed the Q -rise and higher Q_0 values that is typical of high temperature doped cavities reaching a maximum Q_0 of 3.6×10^{10} at $E_{acc} = 16$ MV/m and $T = 2.0$ K. This results in a factor of ~ 1.6 increase in quality factor at this field over the two cavities shown that received only a degas. A hard thermal quench limited the maximum gradient to $E_{acc} = 25$ MV/m and was most likely caused by a defect.

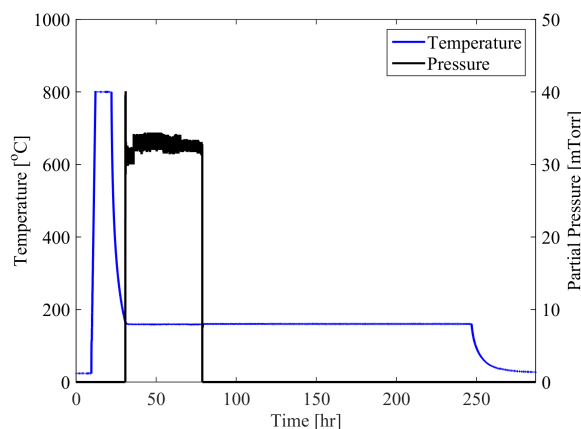


Figure 2: Temperature and pressure profile of the heat treatment of C4P2. Continuously flowing nitrogen gas at ~ 34 mTorr was used for the doping step. The 800 °C degas lasted for 10 hr, the 160 °C doping step was 48 hr, and the 160 °C ultra-high vacuum anneal was 168 hr in length.

A decomposition of the surface resistance, R_S , into temperature dependent, R_{BCS} , and independent components, R_0 , reveals that the Q -rise seen results in a reduction of R_{BCS} with increasing fields while the residual resistance, R_0 , remains relatively constant. This is the same field dependence seen in the resistance of C4P1. The decomposition of the surface resistance for both the low and high temperature doped cavities are shown in Fig. 3.

Two cavities received only degas treatments to establish a baseline performance curve. Cavity C1P1 received a 900 °C bake for 3 hr in vacuum while C1P2 received an 800 °C bake for 5 hr. The so-called ‘medium-field Q -slope’ is apparent in both curves while, due to a low quench field of C1P2, only one displays the ‘high-field Q -slope’ that is typical of cavities with this treatment.

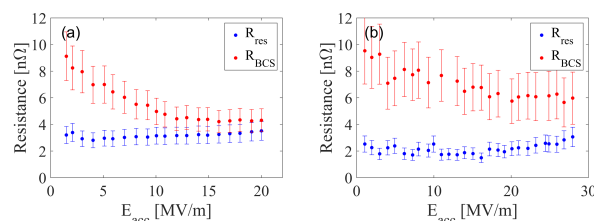


Figure 3: Field dependence of the R_{BCS} and the residual resistance, R_0 , for the low temperature doped cavity, (a), and the high temperature doped cavity, (b).

Content from this work may be used under the terms of the CC BY 3.0 licence (© 2017). Any distribution of this work must maintain attribution to the author(s), title of the work, publisher, and DOI.

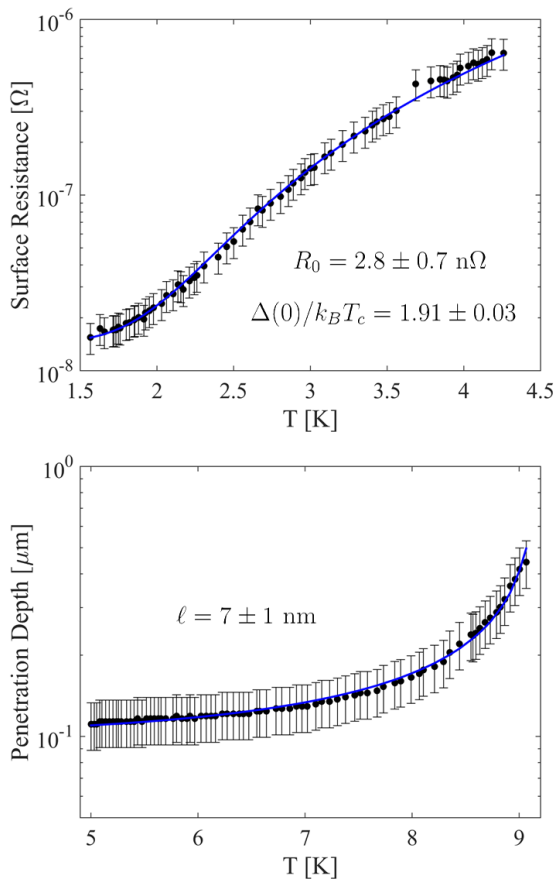


Figure 4: **Top:** Measured penetration depth, λ , vs. T and the BCS fit from the SRIMP code along with the extracted mean free path. **Bottom:** Measurements of the surface resistance, R_S , as a function of T with the BCS fit from SRIMP and the extracted energy gap and residual resistance.

The SRIMP code developed by Halbritter [11] and translated into MATLAB by Valles [12] was used to extract several material properties of the cavities that were tested. Included in the extracted properties were the electron mean free path, ℓ , quasi-particle energy gap, $\Delta(0)/k_B T_c$, and the temperature independent residual resistance, R_0 . The code fits measurements of the penetration depth, λ , as a function of T , to extract ℓ . Both $\Delta(0)/k_B T_c$ and R_0 are extracted from a fit of R_S vs. T . These fits and the extracted parameters for C4P2 are shown in Fig. 4. The extracted mean free path for cavity C4P2 was ~ 7 nm – a very small value. Typical high temperature nitrogen doped cavities have mean free paths that range from a few to 100 nm.

IMPURITY ANALYSIS

Secondary ion mass spectroscopy of a fine grain sample baked along side the low temperature doped cavity reveals high concentrations of carbon and oxygen and relatively low nitrogen concentration compared to a high temperature nitrogen doped sample that received a 10 μm EP post-doping (see Fig. 6). Notice that the concentration of nitrogen in the high temperature doped sample is essentially constant

through the RF penetration layer (i.e. the gray area in Fig. 6) where as the concentration of nitrogen in the low temperature sample drops off quickly to background levels within the layer.

The high temperature nitrogen-doped sample has a concentration of $\sim 7 \times 10^{19}$ atoms/cm³. In the low temperature sample, the oxide layer (i.e. the black shaded area in Fig. 6) which is approximately ~ 5 nm thick contains a maximum of $\sim 6.5 \times 10^{19}$ atoms/cm³. At a depth of 10 nm into the sample the concentration drops off to $\sim 1.7 \times 10^{19}$ atoms/cm³.

The carbon and oxygen abundance at a depth of 10 nm is significantly higher than that of nitrogen in the low temperature doped sample with concentrations of $\sim 9.1 \times 10^{20}$ atoms/cm³ and $\sim 1.5 \times 10^{21}$ atoms/cm³, respectively. At a depth of 50 nm into the sample, the concentrations of carbon and oxygen are both $\sim 4.5 \times 10^{20}$ atoms/cm³.

DIFFUSION MODEL

Fick's second law (Eq. 1) was used as a simple diffusion model for C, N, and O in niobium.

$$\frac{\partial c}{\partial t} = D \frac{\partial^2 c}{\partial x^2}. \quad (1)$$

The impurity concentration, c , depends on the diffusion time, t , and depth in the niobium, x . The diffusion coefficient, D , is dependent on temperature. The solutions to Fick's law with the appropriate boundary conditions is:

$$c(x, t) = C' + (C'' - C') \text{erfc} \left(\frac{x}{2\sqrt{Dt}} \right). \quad (2)$$

where C' is the initial concentration of the impurity throughout the niobium and C'' is the impurity concentration at the surface.

The model is calculated numerically with C' , C'' , and D as fit parameters and takes into account the temperature dependence of D . We assume an instantaneous jump in temperature from 800 to 160 °C as the ramp down period is short compared to the doping step. The diffusion model fits are plotted with the measured impurity concentrations in Fig. 7. The fits agree very well with the measured diffusion curves, demonstrating that even a simple diffusion model describes the diffusion for C, N, and O in Nb quite well in the low and high temperature regime. The resulting diffusion constant fit parameters are shown in Table 3. Care must be taken when comparing these values of D to literature values as interactions between interstitial solute atoms of different species can affect diffusion constants [4].

SAMPLE ANALYSIS

A series of single crystal niobium samples were baked with various recipes (see Table 2) and analyzed with secondary ion mass spectroscopy to determine how temperature and duration affect the concentration profiles of C, N, and O. Figure 5 shows the concentration profiles of samples baked in nitrogen. Each plot corresponds to a different sample. All samples received a 150 μm EP before baking.

Table 2: Single Crystal Sample Treatments

| Sample | EP (μm) | Bake | Gas Purity |
|--------|----------------------|---|------------|
| SC-1 | 150 | — | — |
| SC-2 | 150 | 800 °C (5 hr) | — |
| SC-3 | 150 | 800 °C (5 hr) + 160 °C (48 hr) | — |
| SC-4 | 150 | 800 °C (5 hr) + 160 °C (48 hr; N ₂) | 99.998 % |
| SC-5 | 150 | 800 °C (5 hr) + 160 °C (96 hr; N ₂) | 99.998 % |
| SC-6 | 150 | 800 °C (5 hr) + 160 °C (48 hr; N ₂) | 99.998 % |
| SC-7 | 150 | 800 °C (5 hr) + 160 °C (48 hr; Ar) | 99.999 % |
| SC-8 | 150 | 800 °C (5 hr) + 160 °C (48 hr; Ar) | 99.9999 % |
| SC-9 | 150 | 800 °C (5 hr) + 160 °C (48 hr; Ar + CO ₂) | 99.9999 % |

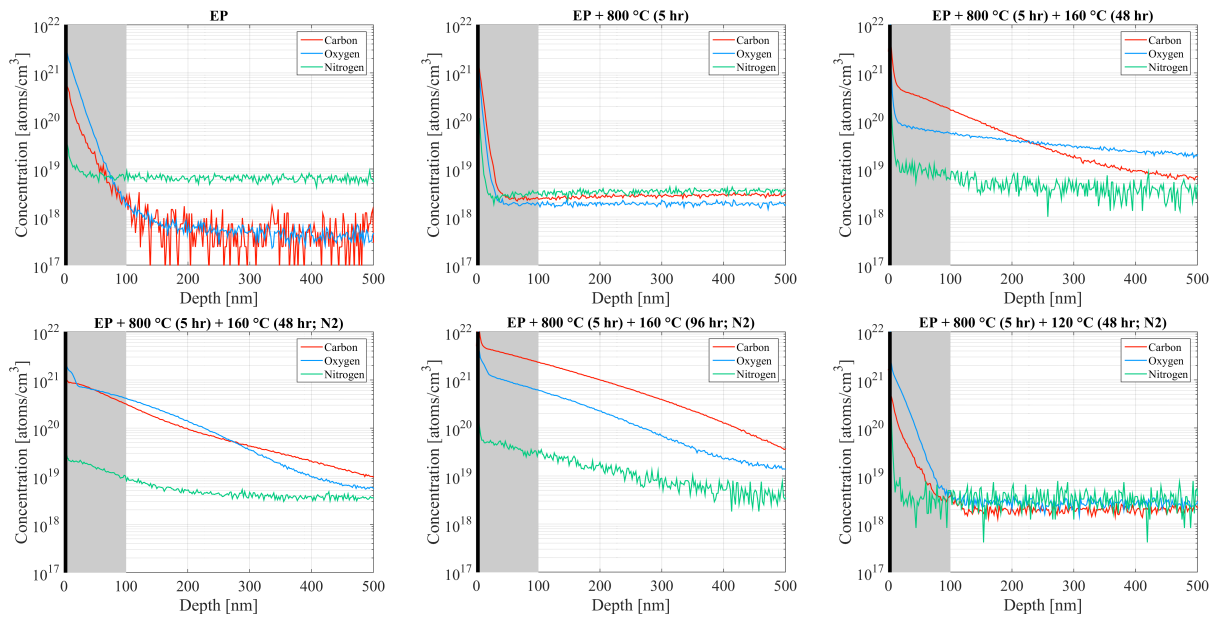


Figure 5: Concentration profiles of C, N, and O in single crystal niobium samples prepared with various nitrogen bakes.

Table 3: Diffusion Model Fit Parameters

| Impurity | D (160 °C) [cm^2/s] | D (800 °C) [cm^2/s] |
|----------|---|---|
| C | 4.7×10^{-17} | 1.5×10^{-13} |
| N | 2.8×10^{-17} | 3.7×10^{-14} |
| O | 4.0×10^{-18} | 6.9×10^{-14} |

Sample SC-1 has relatively high concentrations of C and O within the first 50 nm. However, the concentration profiles for both drop off rapidly to background levels below that of N. The abundance of C and O near the surface could be attributed to the 150 μm EP and 30 min ultrasonic methanol rinse the sample underwent.

The 800 °C bake that sample SC-2 received removed the excess C and O near the surface and slightly lowers the background concentration of N. At 800 °C, high diffusion constants lead to degassing and rapid diffusion into the bulk, accounting for the observed concentration profiles.

Sample SC-3 has increased levels of all three impurities. This is most likely due to the presence of residual gases such

as H₂O, N₂, O₂ and CO₂ in the furnace during the 48 hr vacuum bake at 160 °C.

Adding continuously flowing nitrogen to the 160 °C bake, as can be seen in the concentration profiles of SC-4, increases the abundance of C, N, and O. This is attributed to the higher concentration of impurities in the nitrogen gas used over the furnace background levels. The exact concentrations of trace impurities in all gases used during sample treatments is summarized in Table 4.

Doubling the 160 °C bake time to 96 hr increases the diffusion lengths of all impurities by $\sqrt{2} \sim 1.4$ according to Fick's law which is corroborated by the concentration profiles in Fig. 5. The last sample, SC-6, was baked at 120 °C for 48 hr instead of 160 °C. Comparing to SC-2, we see that the concentration profiles of C and O have similar background levels as is expected at this lower temperature.

Samples SC-7 through SC-9 were degassed at 800 °C for 5 hr followed by a bake at 160 °C for 48 hr with various purity levels of argon gas. SC-7, having the lower overall purity has higher concentrations of both C and O than SC-8. The most significant difference, however, is the difference

Content from this work may be used under the terms of the CC BY 3.0 licence (© 2017). Any distribution of this work must maintain attribution to the author(s), title of the work, publisher, and DOI.

Table 4: Gases Used During Heat Treatments With Impurity Concentrations in ppm

| Gas | Purity (%) | O ₂ | H ₂ O | CO | CO ₂ | THC | N ₂ |
|---|------------|----------------|------------------|-----|-----------------|-----|----------------|
| Nitrogen (High Purity) | 99.998 | 5 | 3 | – | – | – | – |
| Argon (Ultra High Purity) | 99.999 | 1 | 1 | 1 | 1 | 0.5 | 5 |
| Argon (Research Plus) | 99.9999 | 0.1 | 0.2 | 0.1 | 0.1 | 0.1 | 2 |
| Argon (Research Plus) + CO ₂ | 99.9999 | 0.1 | 0.2 | 0.1 | 10 | 0.1 | 2 |

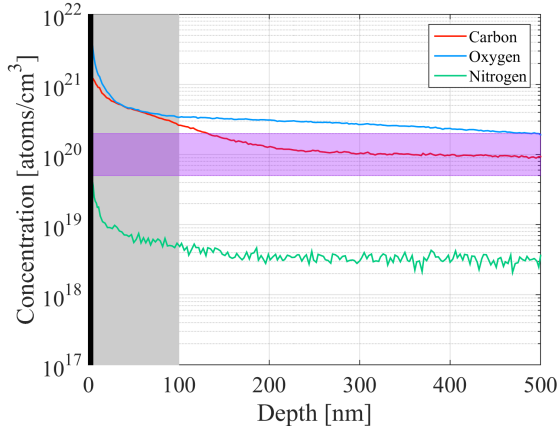


Figure 6: Concentration profiles of C, N, and O for a sample doped at low temperature with the same recipe as C4P2. Typical high temperature (800 °C) nitrogen-doped samples have a concentration profile of N lying in the light purple band after receiving post-doping EP.

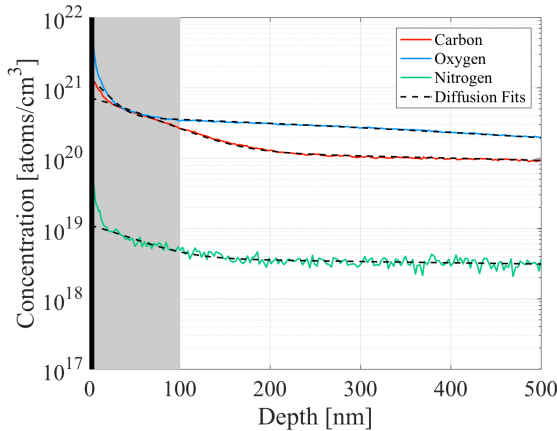


Figure 7: Concentration profiles of C, N, and O for a sample doped at low temperature with the same recipe as C4P2 with the diffusion model fits (dashed black lines).

in concentration in C between the two samples. The abundance of C in SC-7 is higher by about the same factor that concentration CO and CO₂ increases from the research plus to the ultra-high purity gas. Not surprisingly, when 10 ppm CO₂ was added to the research plus argon, the concentration of C increases dramatically.

ANALYSIS

As was seen previously, measurements yielded $\ell \approx 7$ nm for cavity C4P2. In this regime, the penetration depth is ~ 100 nm. For the sake of consistency, we will use the measured concentrations of C, N, and O at a depth of 50 nm to calculate an estimate for the mean free path. At this depth, the concentrations of C and O is $\sim 4.4 \times 10^{20}$ atoms/cm³ corresponding to 0.8 at. % C, O. The concentration of N at 50 nm is $\sim 5.6 \times 10^{18}$ atoms/cm³ and, consequently, can be ignored.

The change in resistivity of niobium due to a concentration, c , of impurity atoms can be calculated using [13]:

$$\Delta\rho = a \cdot c \quad (3)$$

where $a = 4.3 \times 10^{-8} \Omega\cdot\text{m}$ for C and $4.5 \times 10^{-8} \Omega\cdot\text{m}$ for O [14]. This yields $\Delta\rho_C = 3.4 \times 10^{-8} \Omega\cdot\text{m}$ and $\Delta\rho_O = 3.6 \times 10^{-8} \Omega\cdot\text{m}$. The mean free path is then related to the change in resistivity by [2]:

$$\ell = \frac{\sigma}{\Delta\rho_C + \Delta\rho_O} \quad (4)$$

From Goodman and Kuhn [15], $\sigma = 0.37 \times 10^{-15} \Omega\cdot\text{m}^2$ which produces a mean free path estimate of $\ell \sim 5$ nm. This is remarkably close to the measured mean free path of 7 ± 1 nm.

To further rule out N as the cause of the reduction in mean free path, we take its maximum concentration of 0.12 at. % to calculate an estimate of the mean free path. The resulting change in resistivity due solely to the nitrogen at this concentration is $6.0 \times 10^{-9} \Omega\cdot\text{m}$ leading to a mean free path estimate of $\ell \sim 60$ nm — far off from the RF measurement. At a depth of 50 nm, the estimate becomes ~ 712 nm. These facts strongly suggest that C and O play the dominant role in the reduction of the mean free path, ruling out N as a possibility.

CONCLUSION

We have shown that treating niobium in a continuously flowing, low pressure nitrogen atmosphere at low temperatures (120 – 160 °C) introduces interstitial carbon, nitrogen, and oxygen in the niobium lattice. The concentrations of carbon and oxygen were similar to that of high-temperature nitrogen-doped cavities whereas the nitrogen concentration was not significant. This led to a reduction of the electronic mean free path and, consequently, the observed Q -rise and high Q_0 values. Low temperature doping adds the benefit

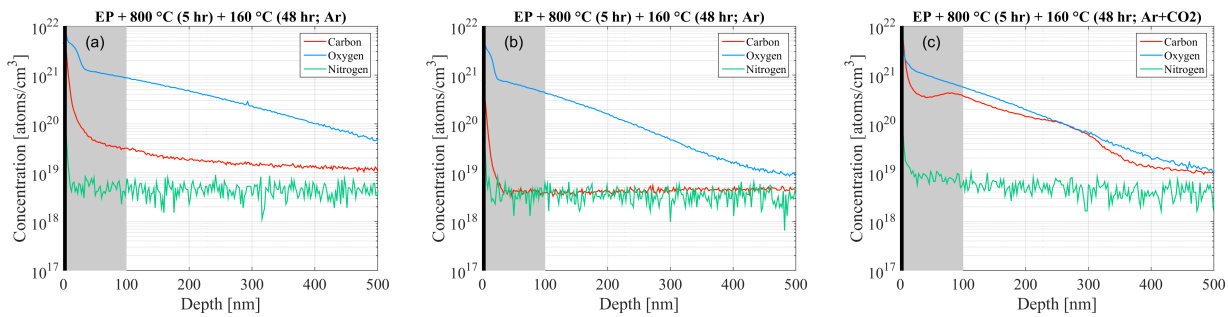


Figure 8: Concentration profiles of C, N, and O in single crystal niobium samples prepared with various bakes using different argon gas mixtures: (a) ultra-high purity argon – 99.999 % purity, (b) research plus argon – 99.9999 % purity, and (c) research plus argon – 99.9999 % purity mixed with 10 ppm CO₂.

of eliminating the need for post-treatment electro-polishing. Further investigation is required to determine sensitivity of the residual resistance to trapped magnetic flux of low temperature doped cavities. Additional cavity RF testing is needed to determine the optimal doping level and procedure.

REFERENCES

- [1] A. Grassellino, A. Romanenko, D. Sergatskov, O. Melnychuk, Y. Trenikhina, A. Crawford, A. Rowe, M. Wong, T. Khabiboulline, F. Barkov, “Nitrogen and argon doping of niobium for superconducting radio frequency cavities: a pathway to highly efficient accelerating structures,” *Supercond. Sci. Tech.*, vol. 26, no. 102001, 2013.
- [2] D. Gonnella, “The fundamental science of nitrogen-doping of niobium superconducting cavities,” Ph.D. dissertation, 2016.
- [3] A. Grassellino and S. Aderhold, “New low T treatment cavity results with record gradients and Q,” in *Proceedings of the TESLA Technology Collaboration, Saclay, France*, 2016.
- [4] R. W. Powers and M. V. Doyle, “Diffusion of interstitial solutes in the group v transition metals,” *J. Appl. Phys.*, vol. 30, no. 4, 1959.
- [5] A. Grassellino, A. Romanenko, Y. Trenikhina, M. Checchin, M. Martinello, O. S. Melnychuk, S. Chandrasekaran, D. A. Sergatskov, S. Posen, A. C. Crawford, S. Aderhold, D. Bice, “Unprecedented quality factors at accelerating gradients up to 45 mv/m in niobium superconducting resonators via low temperature nitrogen infusion,” 2017, arXiv:1701.06077.
- [6] P. N. Koufalas, D. L. Hall, M. Liepe, and J. T. Maniscalco, “Effects of interstitial carbon and oxygen on niobium superconducting cavities,” 2017, arXiv:1612.08291.
- [7] B. Aune *et al.*, “Superconducting TESLA cavities,” *Phys. Rev. ST Accel. Beams*, vol. 3, no. 092001, 2000.
- [8] A. Gurevich, “Reduction of dissipative nonlinear conductivity of superconductors by static and microwave magnetic fields,” *Phys. Rev. Lett.*, vol. 113, no. 087001, 2014.
- [9] J. T. Maniscalco, M. Liepe, D. Gonnella, “The importance of the electron mean free path for superconducting RF cavities,” *J. App. Phys.*, vol. 21, no. 043910, 2017.
- [10] D. C. Ford, P. Zapol, L. D. Cooley, “First-principles study of carbon and vacancy structures in niobium,” *J. Phys. Chem. C*, vol. 119, no. 26, 2015.
- [11] J. Halbritter, “Fortran-program for the computation of the surface impedance of superconductors,” Karlsruhe, Germany, Tech. Rep., 1970.
- [12] N. Valles, “Pushing the frontiers of superconducting radio frequency science: From the temperature dependence of the superheating field of niobium to higher-order mode damping in very high quality factor accelerating structures,” Ph.D. dissertation, 2013.
- [13] H. Padamsee, J. Knobloch, T. Hays, *RF Superconductivity for Accelerators*, 2nd ed. Wiley, 2008.
- [14] K. K. Schulze, “Preparational characterization of ultra-high purity niobium,” *J. Met.*, vol. 33, 1981.
- [15] B. B. Goodman and G. Kuhn, “Influence of extended defects on the superconductive properties of niobium,” *J. Phys. Paris*, vol. 29, no. 240, 1968.

Content from this work may be used under the terms of the CC BY 3.0 licence (© 2017). Any distribution of this work must maintain attribution to the author(s), title of the work, publisher, and DOI.